



Linear and nonlinear optical properties of a modified Gaussian quantum dot: pressure, temperature and impurity effect

Hossein Bahramiyan^{*,1}, Somayeh Bagheri²

¹ Department of Physics, Marvdasht Branch, Islamic Azad University, Marvdasht, Iran

² Department of Physics, Marvdasht Branch, Islamic Azad University, Marvdasht, Iran

(Received 8 Jun. 2018; Revised 17 Jul. 2018; Accepted 21 Aug. 2018; Published 15 Sep. 2018)

Abstract: In this paper, the effect of pressure, temperature and impurity on the energy levels, binding energy, linear and nonlinear optical properties of a modified Gaussian quantum dot are studied. In this regard, the finite element method is employed to solve the single electron Schrodinger equation in the effective mass approximation with and without impurity at the center of the dot. In addition, the energy levels, the wave functions, binding energy, absorption coefficients and refractive index changes for different pressures and temperatures are calculated. The results show that the energy levels decrease by increasing pressure and increase by increasing the temperature for both, with and without impurity, situations. Also, in the presence of impurity, the refractive index changes are greater than the case without impurity and shift to higher energies. Furthermore, by increasing the pressure, the refractive index changes increase and shift to lower energy for both with and without impurity cases. By increasing the pressure and temperature the absorption coefficients decrease and shift to lower energy for all with and without impurity cases

Keywords: Optical Properties, Modified Gaussian Quantum Dot, Impurity, Temperature and Pressure Effect

1. INTRODUCTION

Semiconductor devices have a fairly long history, although the greatest explosion of technology has occurred during the last decades. In the past few years, study of semiconductor nanostructures, have been attracted by many researchers [1-4]. The electronic and optical properties of quantum dots are greatly affected by the geometrical shape, the material structure and the confined potential caused by the surrounded material. The mathematical shape of this potential mostly depends on the geometric and the method of growing of the dot. Different models for the confinement potential would result dissimilar

* Corresponding author. E-mail: hossein.bahramiyan@gmail.com

theoretical values for the electronic and optical properties of similar structures. It is evident that an appropriate model for a particular structure is the one which produces theoretical results in full agreement with the experimental outcomes. This has motivated many authors, to study the effect of different confinement potentials on the physical properties of nanostructures with different geometry in quantum wells, wires and dots in the last decades [5-9].

The physical properties of nanostructures are also very sensitive to impurities and external effects such as magnetic and electric fields, pressure and temperature. Reports on the optical electronic and transport properties of low-dimensional semiconductor structures under external effects such as temperature, pressure and magnetic field [10-12] and analytical calculation for interband light absorption in a parabolic quantum dot in the presence of electrical and magnetic fields by Atoyán et al. [13], calculation of binding energy of a hydrogenic impurity in quantum well by Bastard [14] and study of the binding energy on impurity position and magnetic field in a quantum dot by Kazariyan et al. [15] are quite interesting. For understanding more about the optical and transport properties of low-dimensional semiconductor structures, references [16-19] are suggested.

The electrical and optical properties of nanostructures with shallow-donor impurities in the low-dimensional semiconductor have attracted many researchers [20-26]. The reports mostly deal with different physical properties caused by the size and geometry, application of electric and magnetic fields, dielectric constant mismatch, position-dependence of the effective mass, hydrostatic pressure and temperature effects.

Effects of hydrostatic pressure on impurity states in a spherical GaAs - Ga_{1-x}Al_xAs quantum dots have been investigated by Perez-Merchancano et al. [27]. The donor impurity states in coupled quantum well wires under hydrostatic pressure and the applied electric field by Tangarife et al. [28], hydrostatic pressure and temperature dependence of correlation energy in a spherical quantum dot by Mahendran and Sivakami [29], temperature effects on electron correlations in two coupled quantum dots by Leino and Rantala [30] and the effect of temperature on the binding energy of the lower excited states in a quantum well by Nithiyanthi and Jaya kumar [31] are interesting reports in the field under consideration.

Usually, a core shell quantum dot approximates by a step potential, but in reality, the confining potential isn't sharp in boundary of core and shell of quantum dot. Due to this point, we use a modified Gaussian potential to describe the confining potential. In this paper the effects of pressure and temperature on the energy levels, binding energy and optical properties of a spherical core-shell quantum dot with a modified Gaussian potential in presence of impurity are investigated. In this regard the Schrödinger equation in the effective mass approximation numerically is solved by using the finite

element method (FEM) and the energy levels, wave functions, and the binding energy the nanostructure without and with a hydrogenic donor impurity under different pressures and temperature are calculated. The results are used to obtain an analytical relation for the optical properties of the system via density matrix approach and an iterative method.

The paper has been organized as: theory and model has been presented in section 2, Optical absorption coefficients and refractive index changes have been discussed in section 3, we have presented in section 4, the numerical results and conclusion have been shown in section 5.

A. Theory and model

In the effective mass approximation, the Hamiltonian of a hydrogenic donor impurity located at the position \mathbf{r}_0 in a quantum dot is given by

$$H = H_0 - \frac{e^2}{\varepsilon(P, T) |\mathbf{r} - \mathbf{r}_0|}, \quad (1)$$

Where

$$H_0 = -\frac{\hbar^2}{2m^*(P, T)} \nabla^2 + V(x, y, z, P, T). \quad (2)$$

Where $m^*(P, T)$ is the effective mass as a function of pressure and temperature (P and T are pressure and temperature respectively) and the indexes w and b are for well ($GaAs$) and barrier ($Al_xGa_{1-x}As$) respectively.

$m_w^*(P, T)$ is such as [32]:

$$m_w^*(P, T) = \frac{m_0}{1 + E_p^\Gamma \left[\frac{2}{E_p^\Gamma(P, T)} + \frac{1}{E_p^\Gamma(P, T) + \Delta_0} \right]} \quad (3)$$

Where m_0 is the free electron mass,

$$E_g^\Gamma(P, T) = E_g^\Gamma(0, T) + bP + cP^2$$

$$E_g^\Gamma(0, T) = 1.519 - \frac{(5.405 \times 10^{-4} T^2)}{(T + 204) \text{ eV}}$$

$$b = 1.26 \times 10^{-2} \frac{\text{eV}}{\text{kbar}} \quad c = -3.77 \times 10^{-5} \frac{\text{eV}}{\text{kbar}}$$

for $GaAs$, and for $Al_xGa_{1-x}As$ ($m_b^*(P, T)$) is $m_b(P, T) = m_w^*(P, T) + 0.083x$ and

$$\begin{aligned} \varepsilon_w(P, T) &= \left\{ 12.74 \exp[-1.73 \times 10^{-3} P] \exp[9.4 \times 10^{-5} (T - 75.6)] T < 200 \right\} \\ \varepsilon_w(P, T) &= \left\{ 12.74 \exp[-1.73 \times 10^{-3} P] \exp[20.4 \times 10^{-5} (T - 300)] T \geq 200 \right\} \end{aligned} \quad (4)$$

Where, $\varepsilon_b(P, T) = \varepsilon_w(P, T) - 3.12x$, and x is the Al mole concentration. In the present work, a spherical core-shell quantum dot, with modified Gaussian confining potential, $V(x, y, z, P, T)$, in the form:

$$V(x, y, z, P, T) = V_0(P, T)(1 - \operatorname{sech}^2(r / R_1)) \quad (5)$$

is considered. Where $r = \sqrt{x^2 + y^2 + z^2}$, R_1 is the core radius of quantum dot and $V_0(P, T)$ is given as [32]:

$$V_0(P, T) = Q \Delta E_g^\Gamma(x, P, T) \quad Q_{C=0.6} \quad (6)$$

Where,

$$\begin{aligned} \Delta E_g^\Gamma(x, P, T) &= \Delta E_g^\Gamma(x) + D(x)P + G(x)T \\ D(x) &= \left[(-1.3 \times 10^{-3})x \right] \frac{eV}{kbar}, \quad G(x) = \left[-(1.11 \times 10^{-3})x \right] \frac{eV}{kbar} \end{aligned}$$

It is clear that, due to the complicated shape of the quantum dot, the calculation of energy levels and wave functions, analytically, is a nontrivial task. Therefore, we are interested in using the finite element method (FEM) to find wave functions and energy levels of the systems [33]. We briefly present the FEM to solve the Schrodinger equation in the Cartesian coordinates in the following.

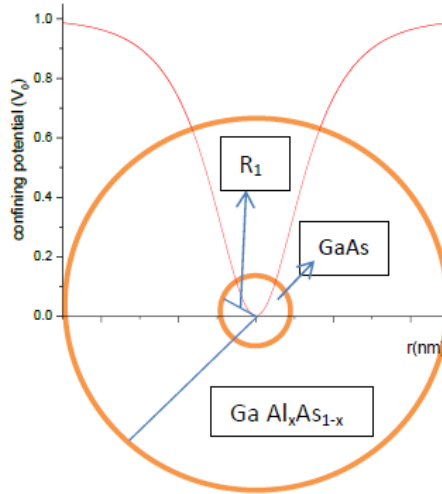


Fig. 1. The boundary surfaces and the shape of a core-shell quantum dot

We consider a volume of some material or materials having known physical properties. The volume represents the domain of a boundary value problem to be solved. We construct a grid in real space using a discrete number of points. The eigen energies and eigen states of the electrons confined in a quantum dot evaluated solving the three dimensional Schrödinger equation

$$\frac{\hbar^2}{2m^*} \left(\frac{\partial^2}{\partial x^2} + \frac{\partial^2}{\partial y^2} + \frac{\partial^2}{\partial z^2} \right) \phi(x, y, z) + (V(x, y, z) + V^{\text{im}}(x, y, z)) \phi(x, y, z) = E \phi(x, y, z) \quad (7)$$

The operator ∇^2 is properly discretized using the standard three-point finite difference approximation. The confined volume is represented by a three-dimensional mesh of (x_i, y_i, z_i) points.

In order to carry out simulation numerically, we need to discretize Eq. (4). The spatial derivative is approximated for all discretized space except on boundaries and given by

$$\begin{aligned}
& \left[\frac{\hbar^2}{2m^*} \left(\frac{\partial^2}{\partial x^2} + \frac{\partial^2}{\partial y^2} + \frac{\partial^2}{\partial z^2} \right) + V(x, y, z) + V^{\text{int}}(x, y, z) \right] \phi^{(\text{in}, \text{out})}(x, y, z) \approx \\
& \frac{1}{\Delta x^2} \left[\phi^{(\text{in}, \text{out})}(i+1, j, k) - 2\phi^{(\text{in}, \text{out})}(i, j, k) + \phi^{(\text{in}, \text{out})}(i-1, j, k) \right] \\
& + \frac{1}{\Delta y^2} \left[\phi^{(\text{in}, \text{out})}(i, j+1, k) - 2\phi^{(\text{in}, \text{out})}(i, j, k) + \phi^{(\text{in}, \text{out})}(i, j-1, k) \right] \\
& + \frac{1}{\Delta z^2} \left[\phi^{(\text{in}, \text{out})}(i, j, k+1) - 2\phi^{(\text{in}, \text{out})}(i, j, k) + \phi^{(\text{in}, \text{out})}(i, j, k-1) \right] \\
& + \left[V(i, j, k) + V^{\text{int}}(i, j, k) \right] \phi^{(\text{in}, \text{out})}(i, j, k)
\end{aligned} \tag{8}$$

$$\text{where } V^{\text{int}}(x, y, z) = \frac{-e^2}{\epsilon |r - r_0|}.$$

The notations $\phi^{(\text{in}, \text{out})}(i, j, k)$ are used as $\phi^{(\text{in}, \text{out})}(i\Delta x, j\Delta y, k\Delta z)$ where $\Delta x, \Delta y$ and Δz are spatial spacing. Also, the wave function inside and outside the dot are represented by the superscriptions "in" and "out" respectively. The continuity of the wave functions on the quantum dot boundary is defined as

$$\phi^{\text{in}}(x, y, z) \Big|_{\text{boundary}} = \phi^{\text{out}}(x, y, z) \Big|_{\text{boundary}} \tag{9}$$

Also, derivative of wave function on the quantum dot boundary is defined as:

$$\frac{1}{m_{\text{in}}} \hat{n} \cdot \nabla \phi^{\text{in}} \Big|_{\text{boundary}} = \frac{1}{m_{\text{out}}} \hat{n} \cdot \nabla \phi^{\text{out}} \Big|_{\text{boundary}} \tag{10}$$

Where \hat{n} is, the normal unite vector of surface boundary. The boundary surfaces and the shape of a core-shell quantum dot have presented in Fig.1.

By applying Eq. (5)-(7), the eigenvalue problem can be rewritten as

$$\begin{bmatrix} A & B \\ C & D \end{bmatrix} \begin{bmatrix} \phi^{\text{in}} \\ \phi^{\text{out}} \end{bmatrix} = E \begin{bmatrix} \phi^{\text{in}} \\ \phi^{\text{out}} \end{bmatrix} \tag{11}$$

where the matrix elements of "A" , "B" , "C" and "D" are the coefficients of ϕ^{in} and ϕ^{out} in Eqs. (5)-(7). The eigenvalues and eigenfunctions of the system can be obtained by diagonalization of matrix of Eq. (8). We use the Flex PDE software to calculate the energy levels and wave functions. Also, the discretization number in any direction is 50 and the convergence check with 0.001 meV error in energy levels. The binding energy (E_b) is given by:

$$E_b = (E_1)_{without\ impurity} - (E_1)_{with\ impurity}, \quad (12)$$

where E_1 is the ground state energy of system.

B. Optical absorption coefficients and refractive index changes

In this section, the refractive index changes and optical absorption coefficients of a spherical quantum dot, caused by an optical intersubband transition are calculated, by using the density matrix formalism where the system is under influence of an electromagnetic field of frequency ω such as:

$$E(t) = Ee^{i\omega t} + E^*e^{-i\omega t}. \quad (13)$$

where E is assumed to be along the z-axis. The time evolution of the matrix elements of one-electron density operator (ρ) can be written as [34, 35]:

$$\frac{\partial \rho}{\partial t} = \frac{1}{i\hbar} [H - qzE(t), \rho] - \Gamma(\rho - \rho^{(0)}), \quad (14)$$

where q is the electronic charge.

The symbol $[,]$ is the quantum mechanical commutator; $\rho^{(0)}$ is the unperturbed density matrix operator; Γ is the phenomenological operator responsible for the Γ damping due to collisions among electrons, and etc. It is assumed that Γ is a diagonal matrix, and its elements are equal to the inverse of relaxation time τ . To solve Eq. (14), Ahn *et al.* [34] applied the standard iterative method. One can obtain the density matrix elements as below:

$$\frac{\partial \rho_{ij}^{(n+1)}}{\partial t} = \frac{1}{i\hbar} [H_0, \rho^{(n+1)}]_{ij} - \Gamma_{ij} \rho_{ij}^{(n+1)} - \frac{1}{i\hbar} [ez, \rho^{(n)}]_{ij} E(t). \quad (15)$$

After obtaining the density matrix, the electronic polarization $P(t)$ and susceptibility $\chi(t)$ can be determined by:

$$P(t) = \varepsilon_0 \chi(\omega) E e^{i\alpha t} + \varepsilon_0 \chi(-\omega) E^* e^{-i\alpha t} = \frac{1}{V} \text{Tr}(\rho M), \quad (16)$$

Where M is dipole moment matrix with elements such that $M_{ij} = \langle i/z | j \rangle$, ε_0 is the permittivity of free space, and Tr symbol stands for the trace of the matrix. The analytical forms of the linear $\chi^{(1)}$ and the third-order nonlinear $\chi^{(3)}$ susceptibility coefficients can be obtained by using Eqs. (15) and (16). [32, 34, 36]. It is shown that the refractive index changes are related to the real part of the susceptibility [32]:

$$\frac{\Delta n(\omega)}{n_r} = \text{Re} \left[\frac{\chi(\omega)}{2n_r^2} \right], \quad (17)$$

where n_r is the refractive index. The linear and the third-order nonlinear refractive index changes can be obtained as [36]:

$$\frac{\Delta n^{(1)}(\omega)}{n_r} = \frac{\sigma_v e^2 |M_{21}|^2}{2n_r^2 \varepsilon_0} \left[\frac{E_{21} - \hbar\omega}{(E_{21} - \hbar\omega)^2 + (\hbar\Gamma_{12})^2} \right], \quad (18)$$

$$\begin{aligned} \frac{\Delta n^{(3)}(\omega)}{n_r} = & - \frac{\sigma_v e^4 |M_{21}|^2}{4n_r^3 \varepsilon_0} \frac{\mu c I}{\left[(E_{21} - \hbar\omega)^2 + (\hbar\Gamma_{12})^2 \right]^2} \\ & \times \left[4(E_{21} - \hbar\omega) |M_{21}|^2 - \frac{(M_{22} - M_{11})^2}{(E_{21})^2 + (\hbar\Gamma_{12})^2} \right. \\ & \left. \times \left\{ (E_{21} - \hbar\omega) \left[E_{21}(E_{21} - \hbar\omega) - (\hbar\Gamma_{12})^2 \right] - (\hbar\Gamma_{12})^2 (2E_{21} - \hbar\omega) \right\} \right], \quad (19) \end{aligned}$$

where σ_v is the carrier density, μ is the permeability, $E_{ij} = E_i - E_j$ is the energy difference, and $M_{ij} = \langle i/z | j \rangle$ is the electric dipole moment matrix element. Using the Eqs. (18) and (19), one can write the total refractive index changes as:

$$\frac{\Delta n(\omega)}{n_r} = \frac{\Delta n^{(1)}(\omega)}{n_r} + \frac{\Delta n^{(3)}(\omega)}{n_r}. \quad (20)$$

It is also shown that the absorption coefficient $\alpha(\omega)$ is related to the imaginary part of the susceptibility $\chi(\omega)$ as [32]:

$$\alpha(\omega) = \omega \sqrt{\frac{\mu}{\varepsilon_R}} \operatorname{Im}[\varepsilon_0 \chi(\omega)]. \quad (21)$$

The linear and third-order nonlinear absorption coefficients can be written as:

$$\alpha^{(1)}(\omega) = \omega \sqrt{\frac{\mu}{\varepsilon_R}} \left[\frac{\sigma_v e^2 \hbar \Gamma_{12} |M_{21}|^2}{(E_{21} - \hbar\omega)^2 + (\hbar\Gamma_{12})^2} \right], \quad (22)$$

$$\begin{aligned} \alpha^{(3)}(\omega, I) = & -\omega \sqrt{\frac{\mu}{\varepsilon_R}} \left(\frac{I}{2n_r \varepsilon_0 c} \right) \frac{\sigma_v e^4 \hbar \Gamma_{12} |M_{21}|^2}{\left[(E_{21} - \hbar\omega)^2 + (\hbar\Gamma_{12})^2 \right]^2} \\ & \times \left\{ 4|M_{21}|^2 - \frac{(M_{22} - M_{11})^2 \left[3E_{21}^2 - 4E_{21}\hbar\omega + \hbar^2(\omega^2 - \Gamma_{12}^2) \right]}{(E_{21})^2 + (\hbar\Gamma_{12})^2} \right\}, \end{aligned} \quad (23)$$

where c is the speed of light in free space, ε_R is the relative electric permeability and I is the optical intensity of the incident wave given by:

$$I = 2 \sqrt{\frac{\varepsilon_R}{\mu}} |E(\omega)|^2. \quad (24)$$

Therefore, the total absorption coefficient is given as:

$$\alpha(\omega, I) = \alpha^{(1)}(\omega) + \alpha^{(3)}(\omega, I) \quad (25)$$

C. Results and discussions

In this section the numerical results for the energy levels, binding energy, transition energy, linear, nonlinear and total refractive index change and absorption coefficients of a spherical core-shell $GaAs/Ga_{0.5}Al_{0.5}As$ quantum dot with a modified Gaussian confining potential are presented. The calculations are presented for 5 nm core and 25 nm shell radii, without impurity and with impurity at the center. The results for the first four non degenerate energy levels of the dot as a function of temperature, with and without impurity, are shown in Fig.2. As it is seen, that the energy levels with impurity are smaller than those without impurity and they increase as the temperature increases (about 1-3 m eV for different levels.)

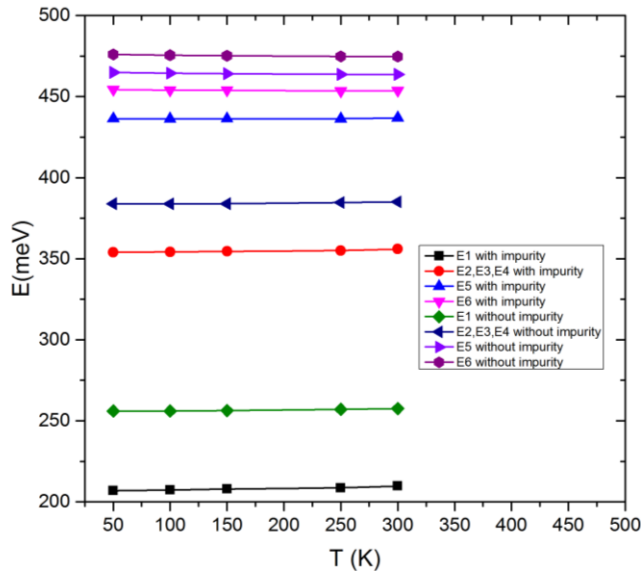


Fig. 2. The first four nondegenerate energy levels with and without impurity as a function of temperature.

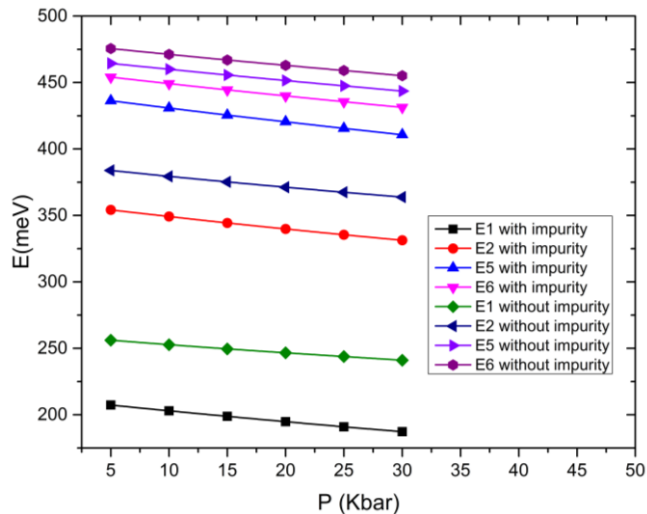


Fig. 3. The first four nondegenerate energy levels with and without impurity as a function of pressure.

Similarly, the first four energy levels were also calculated for different pressures. The results are shown in Fig.3. As it is seen, the energies almost linearly decrease as the pressure increases with the average slope of me V/Kbar.

No appreciate changes in the slope were observed for different energy levels and presence and absence of the impurity.

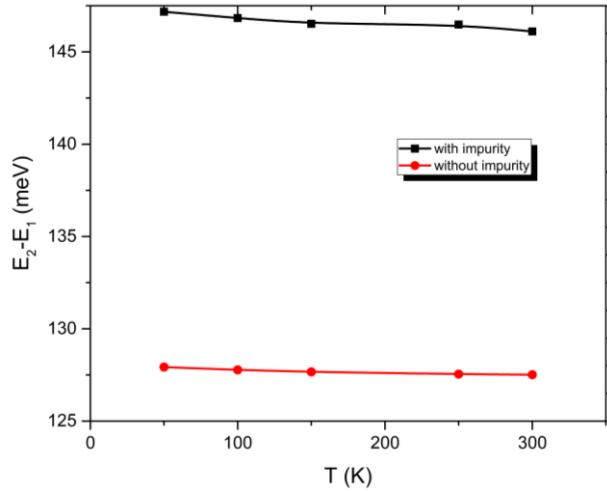


Fig. 4. The energy difference between the first and second energy levels ($E_2 - E_1$) as a function of temperature with and without impurity.

The energy difference between the first and second energy levels ($E_2 - E_1$) as a function of temperature with and without impurity have been shown in Fig.4. The energy difference decreases by increasing the temperature. Also, the energy difference is greater for the dot with impurity. Similar results were observed for ($E_2 - E_1$) as a function of pressure (Fig.5).

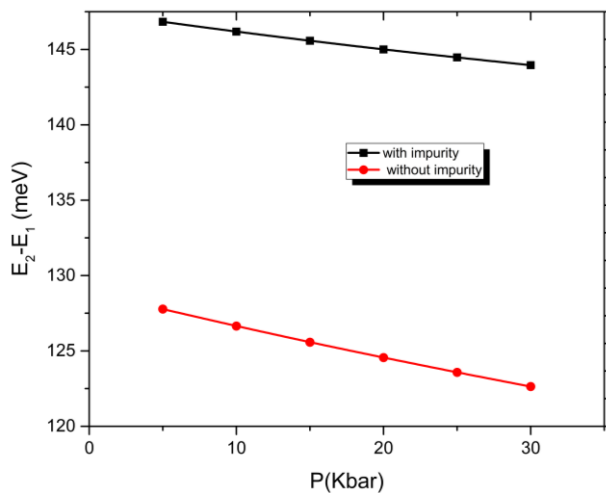


Fig. 5. The energy difference between the first and second energy levels ($E_2 - E_1$) as a function of pressure with and without impurity

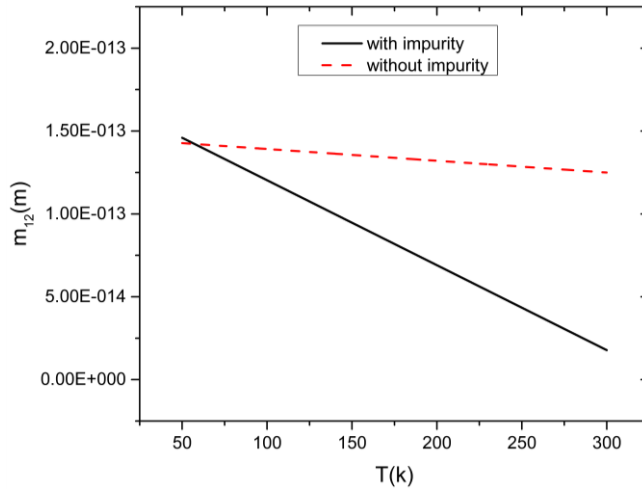


Fig. 6. The dipole matrix element (m_{21}) as a function of temperature with and without impurity.

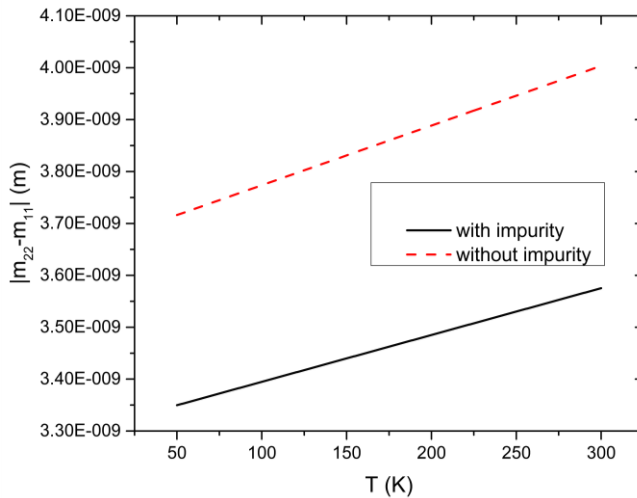


Fig. 7. The dipole matrix element ($|m_{22}-m_{11}|$) as a function of temperature with and without impurity.

We have shown the dipole matrix elements (M_{21}) and ($|M_{22}-M_{11}|$) as a function of temperature with and without impurity in figures 6 and 7 respectively. The dipole matrix elements (M_{21}) decrease by increasing the temperature. Also, the behavior of these matrix elements as a function of pressure with and without impurity, have been shown in figures 8 and 9. The dipole matrix elements (M_{21}) increase by increasing the pressure.

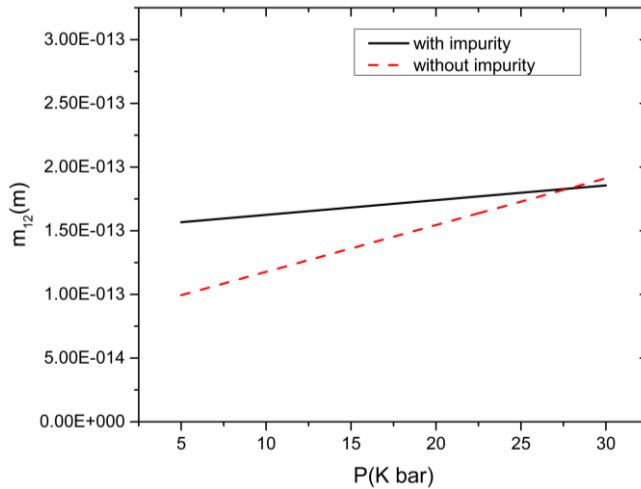


Fig. 8. The dipole matrix element (m_{21}) as a function of pressure with and without impurity.

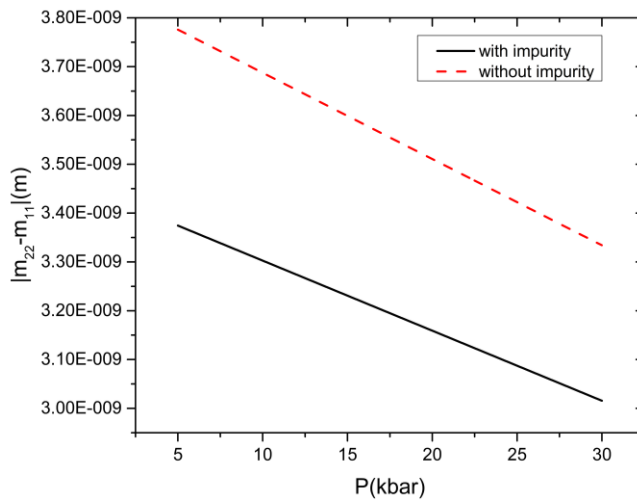


Fig. 9. The dipole matrix element ($|m_{22}-m_{11}|$) as a function of pressure with and without impurity.

The $(|M_{22}-M_{11}|)$ with and without impurity increase by increasing the temperature, and decrease by increasing the pressure. Figures 10 and 11, show the linear and nonlinear absorption coefficients, as a function of photon energy with and without impurity for different pressure, respectively. In the presence of impurity, the absorption coefficients are greater and shift to higher energy. Also,

by increasing the pressure, the absorption coefficients decrease and shift to lower energy for both cases.

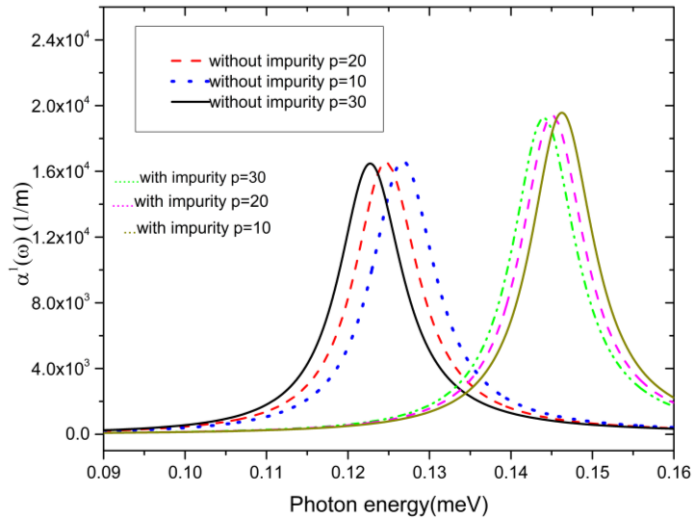


Fig. 10. Linear absorption coefficient, as a function of photon energy with and without impurity for different pressure ($P=10, 20, 30$ kbar).

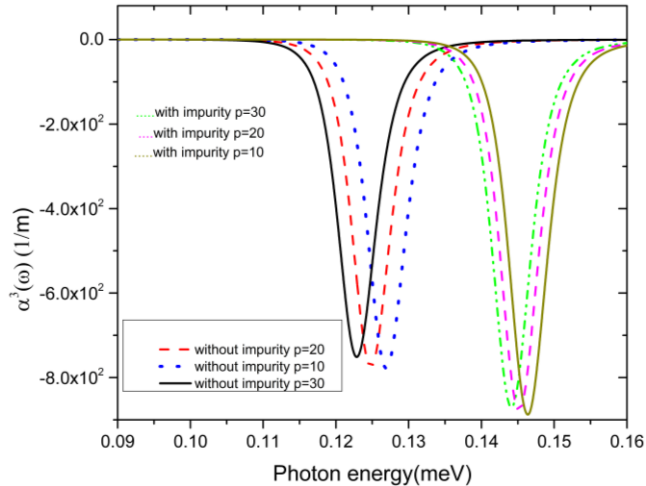


Fig. 11. Nonlinear absorption coefficient, as a function of photon energy with and without impurity for different pressure ($P=10, 20, 30$ kbar).

The linear and nonlinear refractive index changes, as a function of photon energy with and without impurity for different pressure, have been presented in Figs. 12 and 13, respectively. The refractive index changes are greater and shift to higher energy with impurity. Also, the refractive index changes increase and shift to lower energy for both cases, by increasing the pressure.

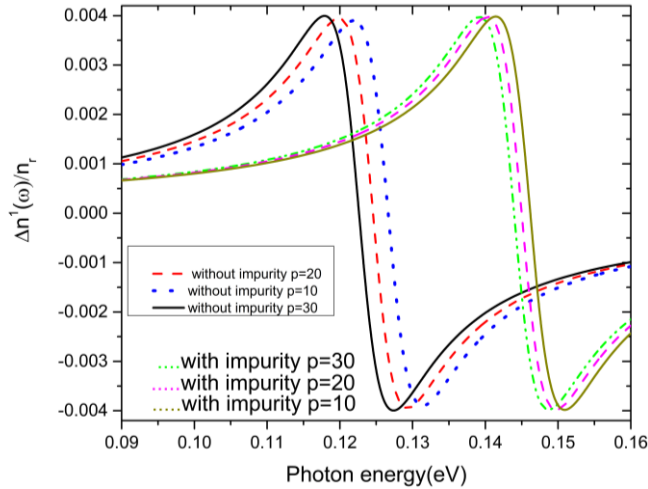


Fig. 12. Linear refractive index change, as a function of photon energy with and without impurity for different pressure ($P=10, 20, 30$ kbar).

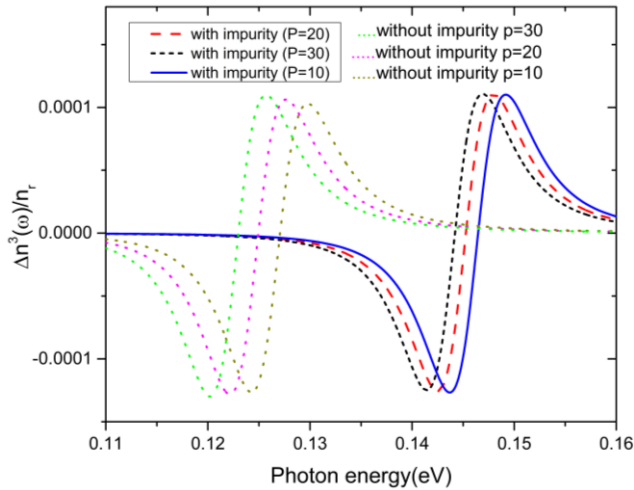


Fig. 13. Nonlinear refractive index change, as a function of photon energy with and without impurity for different pressure ($P=10, 20, 30$ kbar).

The linear and nonlinear absorption coefficients, as a function of photon energy with and without impurity for different temperatures, have been shown in Figs. 14 and 15, respectively. In the presence of impurity, the absorption coefficients are greater and shift to higher energy. Also, by increasing the temperatures, the absorption coefficients decrease and shift to lower energy for all with and without impurity cases.

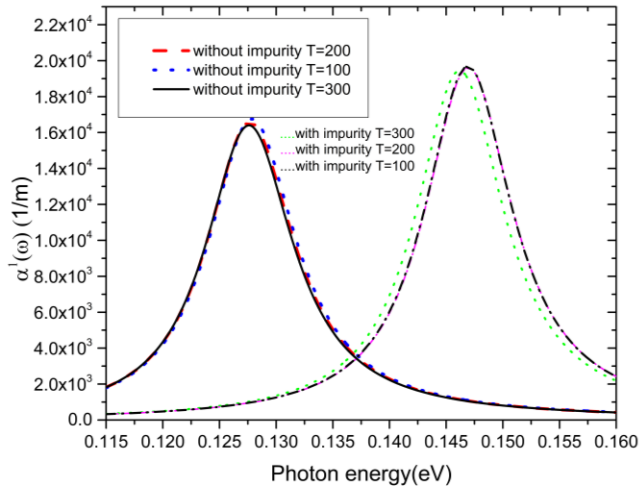


Fig. 14. Linear absorption coefficient, as a function of photon energy with and without impurity for different temperature ($T=100, 200, 300$ K).

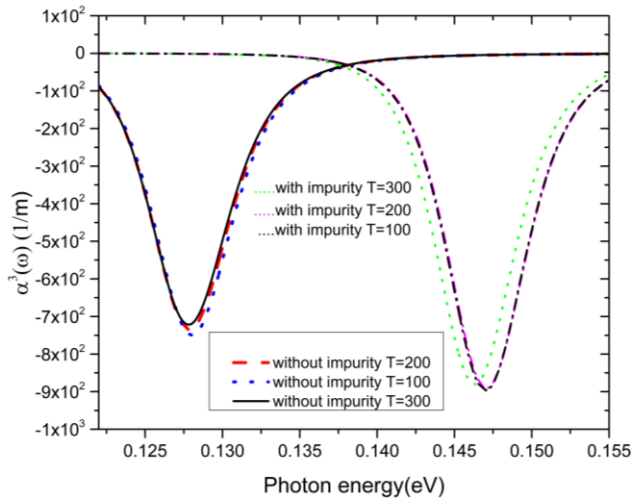


Fig. 15. Nonlinear absorption coefficient, as a function of photon energy with and without impurity for different temperature ($T=100, 200, 300$ K).

Figs. 16 and 17 show the linear and nonlinear refractive index changes, as a function of photon energy with and without impurity for different temperatures, respectively. When system has impurity, the refractive index changes shift to higher energy and are greater. Also, the refractive index changes decrease and shift to lower energy for all with and without impurity cases, by increasing the temperatures

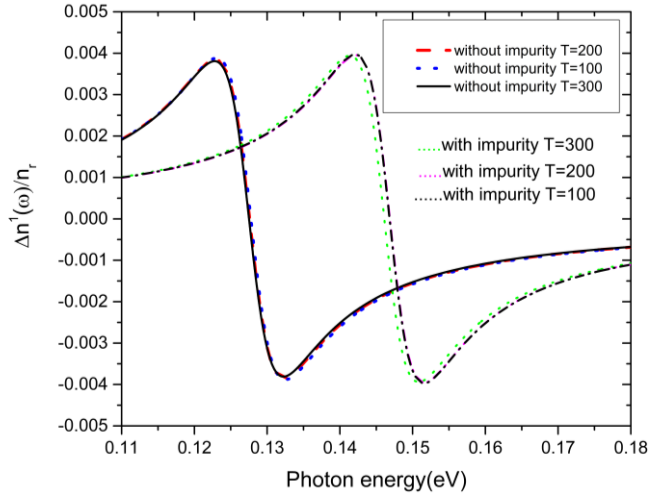


Fig. 16. Linear refractive index change, as a function of photon energy with and without impurity for different temperature ($T=100, 200, 300\text{ K}$).

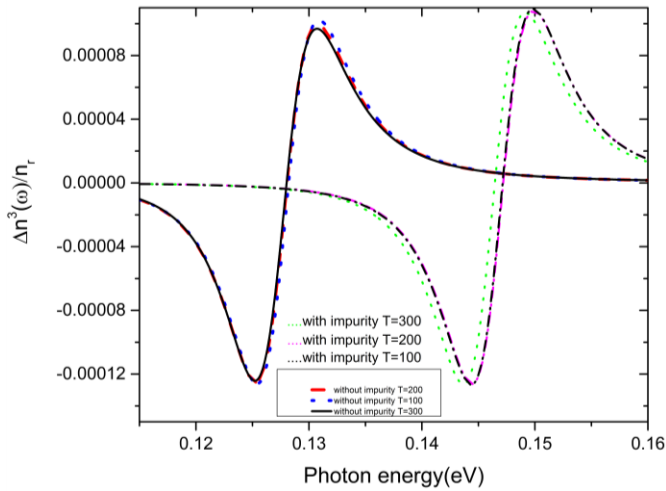


Fig. 17. Linear refractive index change, as a function of photon energy with and without impurity for different temperature ($T=100, 200, 300\text{ K}$).

D. Conclusions

In this paper, we have presented the electronic energy levels, binding energy, linear and nonlinear absorption coefficients and refractive index changes of a modified Gaussian quantum dot with and without impurity. It is clear that the physical properties of a dot are greatly affected by the confined potential caused

by the surrounded material. Different models for the confinement potential would result dissimilar theoretical values for similar structures. It is evident that an appropriate model for a particular structure is the one, which produces theoretical results in full agreement with the experimental outcomes. This has motivated us to study the effect of modified Gaussian confined potential on the physical properties of a spherical quantum dot of GaAs/Ga_{1-x}Al_xAs.

In addition, we have investigated the pressure and temperature effects on the electronic properties. For this purpose, we have calculated the state functions and state energies in the presence of an impurity, for different pressures and temperatures, numerically by using an iterative finite element method in the effective mass approximation. We have also presented the analytical equation for optical properties of the dot by using density matrix approach and an iterative method. The results show that the energy levels decrease by increasing pressure and increase by increasing the temperature for both, with and without impurity, situations. Also, in the presence of impurity, the refractive index changes are greater than the case without impurity and shift to higher energies. Furthermore, by increasing the pressure, the refractive index changes increase and shift to lower energy for both with and without impurity cases. By increasing the pressure and temperature the absorption coefficients decrease and shift to lower energy for all with and without impurity cases.

REFERENCES

- [1] D. K. Ferry and S. M. Goodnick, *Transport in Nanostructures* (Cambridge University Press, Cambridge, UK, 1997).
- [2] Y. Imry, *Introduction to Mesoscopic Physics* (Oxford University Press, Oxford, UK, 1997).
- [3] M. Bouhassoune, R. Charrouf, M. Fliyou, D. Bria, and A. Nougouai, *Polaronic and magnetic field effects on the binding energy of an exciton in a quantum well wire*. J. Appl. Phys, 91 (2002) 232.
- [4] A. I. Ekimov and A. A. Onushchenko, *Quantum size effect in three-dimensional microscopic semiconductor crystals*. JETP Lett. 34 (1981) 345.
- [5] R. Khordad, *Effect of pressure on spin-orbit interaction in a quantum wire with V-shaped cross section*. Solid State Sci. 19 (2013) 63.
- [6] A. Gharaati and R. Khordad, *A new confinement potential in spherical quantum dots: Modified Gaussian potential*. Superlatt. Microstruct. 51 (2012) 194.

- [7] R. Khordad, *Pressure effect on optical properties of modified Gaussian quantum dots*. Physica B, 407 (2012) 1128.
- [8] M. Lu, X. J. Yang, S. S. Perry, J. W. Rabalais, *Self-organized nanodot formation on MgO (100) by ion bombardment at high temperatures*. Appl. Phys. Lett. 80 (2002) 2096.
- [9] P. Nandakumar, C. Vijayan, Y. V. G. S. Murti, *Optical absorption and photoluminescence studies on CdS quantum dots in Nafion*. J. Appl. Phys. 91 (2002) 1509.
- [10] L. Yan, J. Seminario, *Electron transport in Nano-Gold–Silicon interfaces*. J. Quantum Chem. 107 (2007) 440.
- [11] I. Lazic, Z. Ikonic, V. Milanovic, R. W. Kelsall, D. Indjin, P. Harrison, *Electron transport in n-doped Si/SiGe quantum cascade structures*. J. Appl. Phys. 101 (2007) 93703.
- [13] M. S. Atoyan, E. M., *Interband light absorption in parabolic quantum dot in the presence of electrical and magnetic fields*, 31 (2006) 83.
- [12] Kazaryan, H. A. Sarkisyan, *Interband light absorption in parabolic quantum dot in the presence of electrical and magnetic fields*. Phys E, 31 (2006) 83.
- [14] G. Bastard, *Hydrogenic impurity states in a quantum well: A simple model*. Phys. Rev. B, 24 (1981) 4714.
- [15] E. M. Kazaryan, A. V. Meliksetyan, L. S. Petrosyan, H. A. Sarkisyan, *Impurity states of narrow-gap semiconductor parabolic quantum dot in the presence of extremely strong magnetic field*. Phys. E, 31 (2006) 228.
- [16] J. V. Crnjanski, D. M. Gvozdic Serbian, *Self-Consistent Treatment of V-Groove Quantum Wire Band Structure in Nonparabolic Approximation*. J. Electr. Eng, (2004) 69.
- [17] D. S. Chuu, C. M. Hsiao, W. N. Mei, *Hydrogenic impurity states in quantum dots and quantum wires*. Phys. Rev. B, 46 (1992) 3898.
- [18] J. L. Zhu, *Exact solutions for hydrogenic donor states in a spherically rectangular quantum well*. Phys. Rev. B, 39 (1988) 8780.
- [19] S.G. Jayam, K. Navaneethkrishnan, *Effects of electric field and hydrostatic pressure on donor binding energies in a spherical quantum dot*. Solid State Commun, 126 (2003) 681.

- [20] E. Kasapoglu, H. Sari, I. Sokmen, *Geometrical effects on shallow donor impurities in quantum wires*. Phys.E, 19 (2003) 332.
- [21] V. N. Mughnetsyan, M. G. Barseghyan, A. A. Kirakosian, *Stark effects on bound polarons in polar cylindrical quantum wires with finite confining potential*. Superlattices Microstruct, 44 (2008) 86.
- [22] A. Bilekkaya, S. Aktas, S. E. Okan, F. K. Boz, *The electronic properties of a coaxial square GaAs/Al_xGa_{1-x}As quantum well wire in an electric field*. Superlattices Microstruct, 44 (2008) 96.
- [23] R. Khordad, *Electronic properties of two interacting electrons in a quantum pseudodot under magnetic field: Perturbation theory and two parameters variational procedure*. Phys. E, 62 (2013) 166.
- [24] E. Kasapoglu, F. Ungan, H. Sari, I. Sokmen, *The hydrostatic pressure and temperature effects on donor impurities in cylindrical quantum wire under the magnetic field*. Phys. E, 42 (2010) 1623.
- [25] P. Villamil, *Donor in cylindrical quantum well wire under the action of an applied magnetic field*. Phys. E, 42 (2010) 2436.
- [26] R. Khordad, *Effect of pressure on spin-orbit interaction in a quantum wire with V-shaped cross section*. Solid State Sci, 19 (2013) 63.
- [27] S.T. Perez-Merchancano, R. Franco, J. Silva-Valencia, *Impurity states in a spherical GaAs-Ga_{1-x}Al_xAs quantum dots: Effects of hydrostatic pressure*. Microelectron. J, 39 (2008) 383.
- [28] E. Tangarife, M.E. Mora-Ramos, C.A. Duque, *Hydrostatic pressure and electric field effects and nonlinear optical rectification of confined excitons in spherical quantum dots*. Superlatt. Microstruct. 49 (2011) 275.
- [29] A. Sivakami, M. Mahendran, *Hydrostatic pressure and temperature dependence of correlation energy in a spherical quantum dot*. Superlatt. Microstruct, 47 (2010) 530.
- [30] N. Leino, T.T. Rantala, *Temperature Effects on Electron Correlations in Two Coupled Quantum Dots*. Few-Body Syst, 40 (2007) 237.
- [31] P. Nithiananthi, K. Jayakumar, *Effect of temperature on the binding energy of low lying excited states in a quantum well*. Phys. B, 17 (2003) 5811.
- [32] M. J. Karimi, G. Rezaei, M. Nazari, *Linear and nonlinear optical properties of multilayered spherical quantum dots: effects of geometrical size, hydrogenic impurity, hydrostatic pressure and temperature*. Journal of Luminescence, 145 (2014) 55.

- [33] F. S. Levin and J. Shertzer, *Finite-element solution of the Schrödinger equation for the helium ground state*. Phys. Rev. A, 32(1985) 3285.
- [34] D. Ahn, S. L. Chuang, *Calculation of linear and nonlinear intersub band optical absorptions in a quantum well model with an applied electric field*. IEEE J. Quant. Electron, 23 (1987) 2196.

